Accurate Calculation of Stratified Ground Low-Frequency Return Impedance

Karolina Kaszás-Lažetić, Dragan Kljajić, Nikola Djurić and Miroslav Prša

Faculty of Technical Sciences, University of Novi Sad
Trg D. Obradovića 6, 21000 Novi Sad, Serbia
e-mail: kkasas@uns.ac.rs, dkljajic@uns.ac.rs, ndjuric@uns.ac.rs, prsa@uns.ac.rs

Abstract: This paper presents the analytical and numerical calculations of the current distribution and impedance per unit length in real, multi-layer and two-layer homogeneous grounds. Realistic situations consisting of different thicknesses of ground layers were considered in these calculations. Combinations of parameters were considered at frequencies between 50 Hz and 2500 Hz (the 50^{th} harmonic, of the basic frequency). Calculations were conducted by applying a software tool developed previously for a homogeneous ground, based on a combination of analytical and numerical mathematical procedures and modified, using boundary conditions. The problem was also solved numerically by applying the COMSOL Multiphysics software package, based on FEM. The results are validated by comparing them with the results obtained from empirical formulae applied in practical cases.

Keywords: Stratified ground; Two-layer soil; Current distribution; Ground return impedance; Poynting vector flux

1 Introduction

The probability of current, in the ground, is quite high, in all systems for electrical energy transmission and distribution. In power electrical theory and practice, current can be an essential part of the system, as in the case of a single-wire-earth-return, or it can occur by accidental ground faults, lightning strikes or utility overvoltage. In most cases only low frequencies appear in the ground, given the basic industrial frequency and several higher harmonics, and it is of great importance to be well acquainted with both the current distribution in the ground and with the ground impedance.

On the other hand, depending on the electromagnetic sources, that produce current in the ground, time variations of the current could be rapid, so electromagnetic transients and fast transients should be studied as well. In this case, the

electromagnetic field cannot be treated as quasi-static; instead, electromagnetic wave equations have to be applied to determine Transverse Electromagnetic (TEM) waves or quasi TEM waves. Those cases deal with frequencies up to several tenths or hundreds of a MHz.

In order to find an accurate solution for practical problems dealing with the optimization of power transmission and distribution grounding systems, in this paper, only the first case (low frequency, quasi-static electromagnetic fields), is investigated.

For the case of lumped parameters (grounding resistors, capacitors and inductors) applications, which are frequently defined and applied in the power engineering practice, the results could be less accurate, especially in the presence of higher harmonics.

Some of practical approaches have used the concept of the simplified soil model, in which the empirical formulae and diagrams are usually applied. These methods could be efficient in most usual problems, but could also cause significant inaccuracies in applied calculations.

Our first attempt to determine return parameters of low-frequency transmission lines deals with homogeneous soil as the current conducting media. The problem has been identified and calculated in a number of ways that can be classified into three main groups. All the methods, together with their classifications and results are described in detail in [5].

Stratified ground is also the subject of several papers, but mostly at higher frequencies [2] [10] [11] [12]. This is expected given that, in nature, the soil layer thickness is usually much smaller compared to the penetration depth of the low frequency electromagnetic fields. Nevertheless, most of the mentioned papers describe the behavior of the multi-layer soil at a higher frequency range, from 50 Hz to 1 MHz, and only a few contributions at extra low frequencies for homogeneous soil were found in [8].

This paper's significant contribution is the new approach, based on the Poynting theorem, partially presented in [5], improved and successfully adjusted for a multi-layer ground analysis. The developed method takes into account all existing parameters, including soil layer thickness, soil layer resistivity values, conductor height and operational frequency. The other novelty in this paper is the introduction of the third coordinate system to define and apply boundary conditions necessary for an analytical calculation of the electromagnetic field in the case of stratified ground. The proposed procedure has not been used elsewhere in the explored references. Some initial results in the current distribution calculation inside a two-layer soil are given in [3] [4], while some of the other authors' results dealing with multi-layer soils are presented in [7] [13] [16].

The paper consists of three main parts. Section 1 provides background information about the problem, and points out the importance of the new method. Section 2

provides insight into the model geometry and explains the application of the proposed method to multilayer soil. Section 3 presents the most significant results, while the conclusion emphasizes the most important achievements.

2 Theoretical Approach

For the stratified soil return impedance determination, we assume the same system adopted in [5] and depicted in Figure 1; the system contains an overhead conductor that is parallel to the ground surface, with ground serving as a return conductor. The problem could be treated as two-dimensional, in a plane that is perpendicular to the overhead conductor (*x*-*y* plane, *A*–*A* crossing).

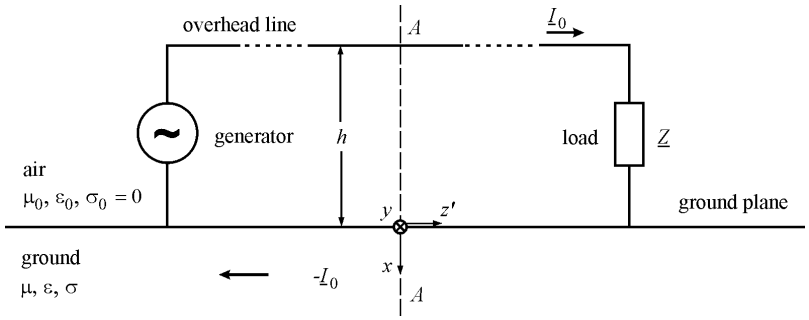

Figure 1
The principle of the ground as a return conductor

In the investigated case of stratified ground, the earth is assumed to have an infinite cross-section, with *n* layers of generally different thicknesses and generally different electromagnetic parameters, cf. Figure 2, for the *A*–*A* crossing.

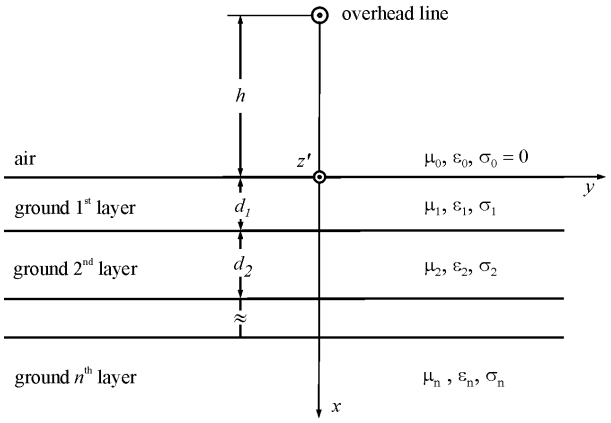

Figure 2
Overhead line over a multi-layer ground

The multi-layer ground conducts the current $-\underline{I}_0$ from the load impedance $\underline{Z}$ towards the generator. Due to the skin effect and the proximity effect with the overhead conductor, and due to the presence of layers with different conductivity values, the current density vector is not uniformly distributed across the infinite cross-section. In homogeneous soil, the current density's maximal magnitude appears under the overhead conductor $(x, y) = (0, 0)$ and decreases with the increasing distance. This maximal value depends on the height of the overhead conductor h, the current frequency f, permeability μ and soil conductivity σ.

In the multi-layer soil case, depending on the layer conductivity values, the maximal current density magnitude is expected to appear at the same point or at the upper boundary between the two neighboring layers.

Adopting the standard analytical approach to the ground return impedance determination, the complex Poynting vector, $\underline{\boldsymbol{P}} = \underline{\boldsymbol{E}} \times \underline{\boldsymbol{H}}^*$, where $\underline{\boldsymbol{E}}$ is the complex electric field strength vector and $\underline{\boldsymbol{H}}^*$ is the conjugate complex magnetic field strength vector, needs to be calculated. From the determined complex Poynting vector, the ground return impedance per unit length, $\underline{Z}'_{\mathrm{G}}$ can then be calculated as (cf. [14]),

$$\underline{Z}'_{\mathrm{G}} = \frac{1}{\left|\underline{I}_0\right|^2} \cdot \int_S \left(\underline{\boldsymbol{E}} \times \underline{\boldsymbol{H}}^* \right) \cdot \mathrm{d}\boldsymbol{S} \,. \tag{1}$$

The analytical integration of the above integral can be difficult to perform, but the sufficiently accurate solution can be derived by numerical integration.

The determination of the current distribution within the ground, taking into account soil stratification, is the starting point for the calculation of the magnetic field strength vector. For this reason, the first step should be the determination of the electric field strength vector.

2.1 Calculation of the Electric Field Strength Vector within any Homogeneous Media

In order to solve the problem within a stratified soil, the partial differential equation in homogenous soil should be solved first. For this reason, a geometric representation of the problem defined by cross section $A - A$ in Figure 1 is presented in Figure 3 also adopted in [5].

First of all, an adequate coordinate system has to be chosen. According to the problem geometry, the cylindrical coordinate system (r, φ, z) is adopted. In the chosen coordinate system, the z-axis runs along the overhead conductor. Both the electric field strength vector and current density vector have only z components, depending on the radius r.

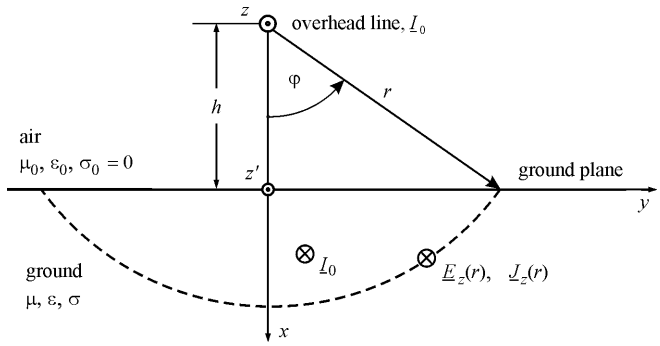

Figure 3
Definition of the chosen coordinate systems for the electric field strength vector calculation

The entire calculation process for a complex electric field strength vector calculation in homogeneous soil is described in detail in [5]. Starting from the first two Maxwell's equations in a complex domain for a quasi-stationary electromagnetic field, it is shown, that the complex electric field strength vector in the ground is a solution to the partial differential equation in the cylindrical coordinate system [5] [14]:

$$\frac{\partial^2 \underline{E}_z}{\partial r^2} + \frac{1}{r}\frac{\partial \underline{E}_z}{\partial r} - \underline{K}^2 \underline{E}_z = 0 \tag{2}$$

In (2), the complex constant $\underline{K}^2$ is defined as:

$$\underline{K}^2 = \frac{\mathrm{j}\omega\mu\sigma}{\pi}\arccos\frac{h}{r} \tag{3}$$

For the constant value of the coefficient $\underline{K}^2$, (2) is Bessel's equation with the general solution:

$$\underline{E}_z(r) = \underline{A} I_0(\underline{K}r) + \underline{C} K_0(\underline{K}r) \tag{4}$$

According to [1], the complex electric field strength vector is defined as:

$$\underline{E}_z(r) = \underline{C} K_0(\underline{K}r) \tag{5}$$

The function $K_0(\underline{K}r)$ is divided into the real and imaginary part, and the complex electric field strength vector takes the form of:

$$\underline{E}_z(r) = \underline{C}\left[\ker(ar) + \mathrm{j}\,\mathrm{kei}(ar)\right] \tag{6}$$

In the above equation the parameter a is:

$$a = \sqrt{\frac{\omega\mu\sigma}{\pi}\arccos\frac{h}{r}} = \sqrt{\frac{\omega\mu}{\rho\pi}\arccos\frac{h}{r}} \tag{7}$$

In order to determine the complex constant $\underline{C}$, the complex current density vector should be integrated over the ground cross-section, S_{Gcs}, (x-y plane):

$$\underline{I}_0 = \int_{S_{Gcs}} \boldsymbol{J} \cdot \mathrm{d}\,\boldsymbol{S}. \tag{8}$$

The complex constant $\underline{C}$ is a function of frequency f, conductor's height above ground h, and soil resistivity value, ρ.

2.2 Complex Current Distribution inside a Multi - Layer Ground

Although many studies are based on the assumption that ground is homogeneous with a constant conductivity value, in reality the soil is not homogeneous; its conductivity changes from point to point. In practice, ground could be thought of as being composed of several layers with different electromagnetic properties.

To have an adequate soil model, the influence of ground stratification on ground impedance calculation should be taken into account.

The soil characteristics can be represented by an idealized multi-layer model, shown in Figure 2.

The top layer is assumed to have a finite depth d_1 from the surface, conductivity σ_1 and permittivity ε_1. The next layer is also assumed to be finite, of thickness d_2, and is characterized by conductivity σ_2 and permittivity ε_2. The last observed layer is assumed to be infinite, with the corresponding electromagnetic characteristics. Assuming that the investigated ground is not made of a ferromagnetic material, permeability values of all layers are set to be the same as the permeability of air, $\mu_1 = \mu_2 \ldots = \mu_n = \mu_0$. Should a soil layer contain any ferromagnetic material, the corresponding value of permeability must be defined and included in the calculations.

In the case of a multi-layer soil, the complex current density vector calculations are slightly different. The complex electric field strength vector is considered to be parallel to the surface between any two soil layers. The boundary conditions that have to be satisfied are that the complex tangential components of the electric field strength vector must be the same on both sides of the surface that separates the i^{th} and the j^{th} layer:

$$\boldsymbol{n} \times (\boldsymbol{E}_1 - \boldsymbol{E}_2) = 0 \quad \rightarrow \quad \underline{\boldsymbol{E}}_{\text{it}} = \underline{\boldsymbol{E}}_{\text{jt}} = \boldsymbol{i}_z E_z. \tag{9}$$

For this reason, the complex electric field strength vector is the same as in the previous model for homogeneous ground. The complex current density vector also has only the z component and will be calculated from the complex electric field strength vector in each soil layer:

$$\underline{J}_1(r) = \sigma_1 \underline{E}_z(r) \quad \underline{J}_2(r) = \sigma_2 \underline{E}_z(r) \quad \ldots \quad \underline{J}_n(r) = \sigma_n \underline{E}_z(r). \tag{10}$$

In this case, the current density vector depends on coordinates *x* and *y*, and on the conductor height *h*.

2.3 Complex Magnetic Field Strength Vector

The determination of the complex magnetic field strength vector $\underline{\boldsymbol{H}}$ is difficult because of the different current density vector values in each ground layer and the calculation in three coordinate systems. In addition, the resultant magnetic field strength vector is composed of two contributions.

The first contribution is produced by the complex current $\underline{I}_0$ in the overhead conductor. This part of the magnetic field strength vector at an arbitrarily chosen point on the ground surface, T (0, *y*), denoted by $\underline{\boldsymbol{H}}_C$, according to Figure 4, is:

$$\underline{\boldsymbol{H}}_C = \frac{\underline{I}_0}{2\pi r} \boldsymbol{i}_\varphi. \tag{11}$$

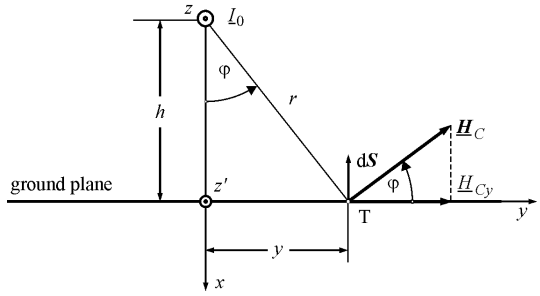

Figure 4
Magnetic field due to the overhead conductor

From (1), it follows that only the *y* component of magnetic field strength vector is relevant, which is:

$$\underline{H}_{Cy} = \frac{\underline{I}_0}{2\pi r}\cos\varphi = \frac{\underline{I}_0}{2\pi r}\frac{h}{h^2 + y^2}, \tag{11}$$

where

$$\cos\varphi = \frac{h}{r} \quad \text{and} \quad r^2 = h^2 + y^2. \tag{12}$$

The current density $\underline{\boldsymbol{J}}_z(r)$ within the ground produces the additional contribution to the magnetic field strength vector $\underline{\boldsymbol{H}}_G$. The resultant *y* component of vector $\underline{\boldsymbol{H}}$ will be the sum of the two parts,

$$\underline{H}_y = \underline{H}_{Cy} + \underline{H}_{Gy}. \tag{13}$$

The magnetic field strength vector produced by the current inside the ground is much more difficult to calculate, due to the fact that the layers are parallel to the surface. For this reason, we decided to determine the complex magnetic field strength vector by applying a mathematical procedure in a Cartesian coordinate system, defined by the axes *x*, *y*, *z'* (see Figure 5).

The complex magnetic field strength vector in an arbitrary point T(0, *y*), on ground surface, produced by the complex current in the ground, can be determined by applying Biot-Savart's law, where:

$$r = |\boldsymbol{r}|, \quad r^2 = d^2 + x'^2 = (y - y')^2 + x'^2, \quad \boldsymbol{r}_0 = \frac{\boldsymbol{r}}{r} = \frac{\boldsymbol{r}}{|\boldsymbol{r}|}. \tag{14}$$

Complex magnetic field strength vector in point T(0, *y*) is then:

$$\underline{\boldsymbol{H}}_{\mathrm{G}}(0, y) = \frac{1}{4\pi}\int_{\mathrm{S}} \frac{\underline{\boldsymbol{J}}(x', y') \times \boldsymbol{r}}{|\boldsymbol{r}|^3}\mathrm{d}S = \frac{1}{4\pi}\int_{\mathrm{S}} \frac{\underline{\boldsymbol{J}}(x', y') \times \boldsymbol{r}_0}{|\boldsymbol{r}|^2}\mathrm{d}S. \tag{15}$$

All quantities in (14) are presented in Figure 5.

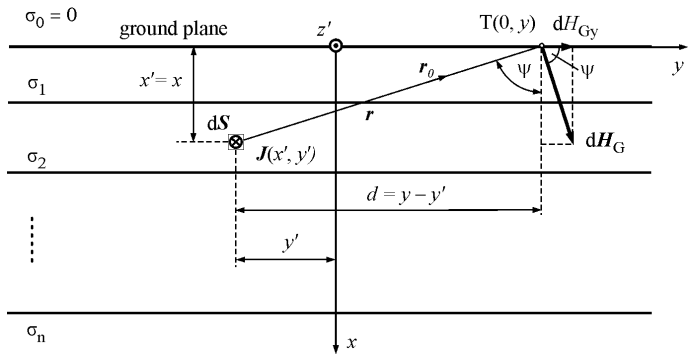

Figure 5

Magnetic field due to the current inside the ground

In order to determine the Poynting vector on the ground surface, the only relevant component of the complex magnetic field strength vector on ground surface is the *y* component:

$$\underline{H}_{\mathrm{Gy}}(0, y) = \underline{H}_{\mathrm{G}} \cos\psi = \frac{1}{4\pi}\int_{\mathrm{S}} \frac{\underline{J}(x', y')}{r^2}\cos\psi \mathrm{d}S = \frac{1}{4\pi}\int_{\mathrm{S}} \frac{\underline{J}(x', y')}{r^2}\frac{x'}{r}\mathrm{d}S. \tag{16}$$

In (16), according to Figure 5, cos ψ is:

$$\cos\psi = \frac{x'}{r} = \frac{x'}{\sqrt{x'^2 + (y - y')^2}}. \tag{17}$$

Hence, in order to calculate the *y* component of the complex magnetic strength field vector, the following surface integral must be solved:

$$\begin{aligned}\underline{H}_{\mathrm{Gy}}(0,y) &= \frac{1}{4\pi}\int_{\mathrm{S}} \frac{\underline{J}(x',y')}{x'^2+(y-y')^2}\frac{x'}{\sqrt{x'^2+(y-y')^2}}\mathrm{dS}= \\ &= \frac{1}{4\pi}\int_{0}^{\infty}\int_{-\infty}^{\infty} \frac{\underline{J}(x',y')}{\sqrt{x'^2+(y-y')^2}}\frac{x'}{\sqrt{x'^2+(y-y')^2}}\mathrm{d}x'\mathrm{d}y'\end{aligned} \tag{18}$$

Knowing that the complex current density vector is a combination of the modified Bessel functions, the integral could be difficult to solve analytically. Nevertheless, this integral could be successfully solved by applying any numerical integration procedure. The integration can be performed on an arbitrarily fine mesh and the obtained results can be very accurate.

Knowing both the complex electric field strength vector $\underline{\boldsymbol{E}}$ and the complex magnetic field strength vector $\underline{\boldsymbol{H}}$, we can calculate the complex Poynting vector and its flux over the ground surface:

$$\underline{\boldsymbol{P}} = \int_{\mathrm{S}} \left(\underline{\boldsymbol{E}} \times \underline{\boldsymbol{H}}^{*}\right)\cdot \mathrm{d}\boldsymbol{S} = \underline{Z}_{\mathrm{G}}\left|\underline{I}_0\right|^2 . \tag{19}$$

Applying (1), the ground return impedance can be calculated.

3 Calculation Results and Discussion

The calculation of current distribution was carried out over several two-layer soils, for four different soil layer resistivity values: $\rho = 1/\sigma$ = 50 Ωm, 250 Ωm, 1000 Ωm and 2500 Ωm, together with five values of the overhead conductor height: h = 10 m, 15 m, 20 m, 25 m and 30 m. In the case of the two-layer soil, several typical combinations of soil resistivity values are calculated. In this paper two of these combinations are presented and discussed.

As most soil types are non-magnetic, the relative permeability of the ground was assumed to be unity, with the relative permittivity also considered equal to one. The Bessel function values necessary for solving (2) were found in [1]. All calculations in frequencies ranging from 50 Hz to 2500 Hz were examined, assuming a sinusoidal current in the overhead conductor, presented in the complex domain as:

$$\underline{I}_0 = (1+\mathrm{j}0)\ \mathrm{kA}. \tag{20}$$

3.1 Current Distribution in a Homogeneous Ground Model

In the case of a homogeneous ground, the entire calculation procedure described with (2) through (9) can be applied to directly determine the current density vector distribution. This procedure, together with the appropriate results, is described in detail in [5]. In this paper some of these results will be repeated for comparison purposes between the homogeneous ground and the multi-layer or the two-layer soil.

The calculated current distribution inside the homogeneous soil, at $\rho = 50$ Ωm and $f = 50$ Hz, for five different conductor heights, is shown in panel (a) of Figure 6, while panel 6 (b) presents the current distribution for a single conductor height of $h = 15$ m, for four different homogeneous soil resistivity values. The diagrams are adopted from [5].

Figure 6 demonstrates that the influence of conductor height on the current distribution within the ground is negligible for the same value of soil resistivity, while the soil resistivity values have a significant impact on the current distribution.

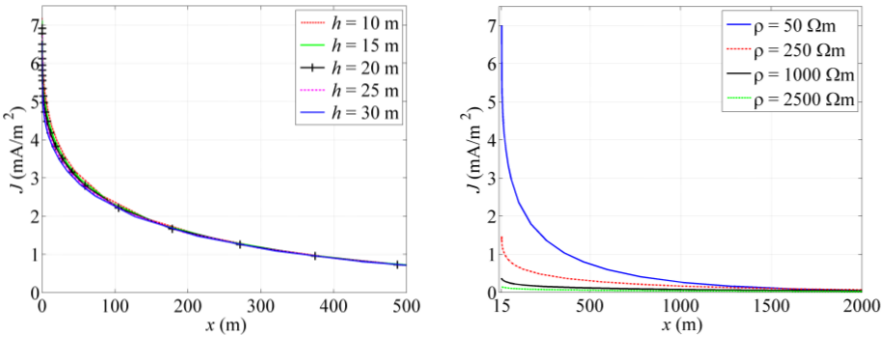

(a) (b)

Figure 6

Current density vector magnitude as a function of overhead conductor height (a) and of soil resistivity values (b)

It is apparent from Figure 6 (b) that the skin effect is the strongest in the case of the smallest soil resistivity value, $\rho = 50$ Ωm, and weakest for the largest soil resistivity value, $\rho = 2500$ Ωm e.g. its influence decreases with increasing soil resistivity. For all four soil resistivity values the current density vector magnitude is the largest at the surface and decreases rapidly with increasing distance from the above conductor.

In the three other cases, i.e. for higher soil resistivity values, the skin effect is less distinct and the penetration depth is much higher.

3.2 Current Distribution in a Multi-Layer Ground Model

As an example of a multi-layer soil, we investigated two-layer soil typical for our region. Typical thicknesses of the layers in our region are 1 m, 2 m and 5 m, with two-layer resistivity combinations presented in Table 1, obtained from local measurements [9].

Table 1
Two-Layer Soil Resistivity Combinations

Layer	ρ [Ωm]						
1	50	50	50	100	100	100	500
2	100	500	1000	1000	3000	50	50

The distribution of current in all combinations of the two-layer soil presented in Table 1 was calculated. In this paper two typical combinations of current distribution are presented and discussed as an example. The corresponding parameters for these combinations are as follows:

- ρ_1/ρ_2 = 50 Ωm/1000 Ωm d_1 =1 m, $d_2 = \infty$
- ρ_1/ρ_2 = 500 Ωm/50 Ωm d_1 =1 m, $d_2 = \infty$

The current distribution for the first soil resistivity combination, at 50 Hz and at 450 Hz, is shown in Figure 7.

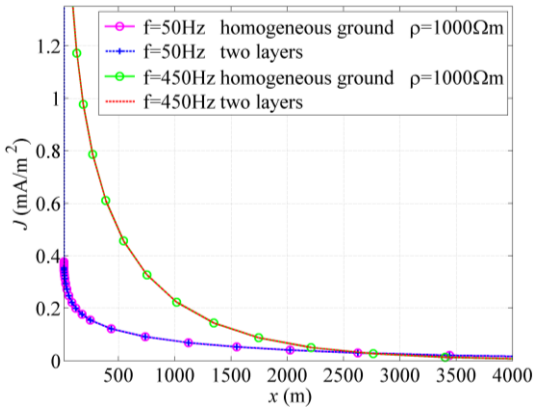

Figure 7
Current distributions inside a two-layer soil, 50 Ωm/1000 Ωm, at 50 Hz and 450 Hz, in a wide range

Due to the negligible thickness of the first layer compared to the overall ground depth, the influence of the soil resistivity values is not visible in Figure 7. Figure 8 depicts a zoomed-in version to the depth of 5 m.

The drop in current density vector magnitude on the boundary that separates the two layers is evident at both frequencies. Due to the less emphasized skin effect at

a lower frequency, the difference between the current density vector magnitudes in a two-layer soil is smaller at 50 Hz. Due to the more significant skin effect, the current density vector magnitude drop is much higher at 450 Hz.

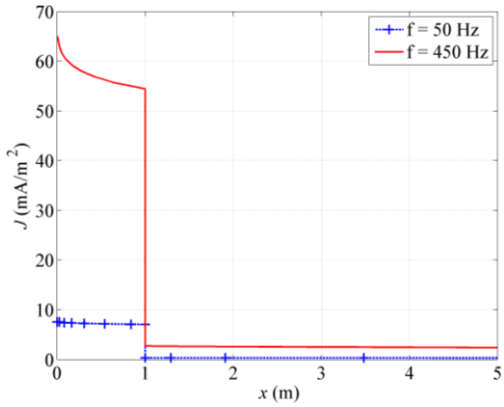

Figure 8

Current distribution inside a two-layer soil, 50 Ωm/1000 Ωm, at 50 Hz and 450 Hz, in a limited range

The same current distribution can also be presented by contour lines and an appropriate color-map. As in Figure 7, the case of current density vector magnitude presentation in a wide range beneath the ground surface, the influence of two different resistivity values cannot be noticed.

For this reason, only the current density vector magnitude distribution to the depth of 10 m is presented in Figure 9. The higher density of contour lines in the upper layer describes the higher current density vector values.

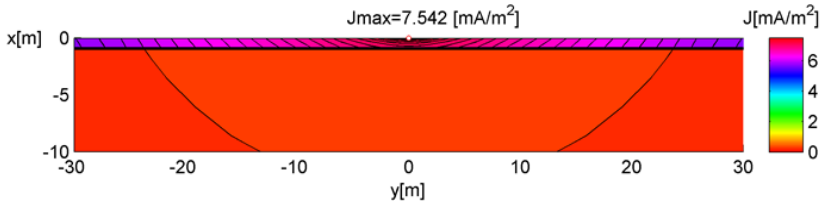

Figure 9

Current distribution inside a two-layer soil, 50 Ωm/1000 Ωm, at 50 Hz, up to the 10 m depth

A similar situation as in the first case, $\rho_1/\rho_2 = 50$ Ωm/1000 Ωm, appears in the second case, $\rho_1/\rho_2 = 500$ Ωm/50 Ωm as well. When the calculated current distribution is presented in a wide range beneath the ground surface, the influence of two layers with different soil resistivity values is negligible, again due to the negligible thickness of the first layer, comparing to the observed ground depth. For this reason, the results are presented in two diagrams; in a wide ground range and in a limited range beneath the ground surface.

Current distribution for the second case of the two-layer ground is presented in Figure 10, while the same results on a zoomed-in region are presented in Figure 11.

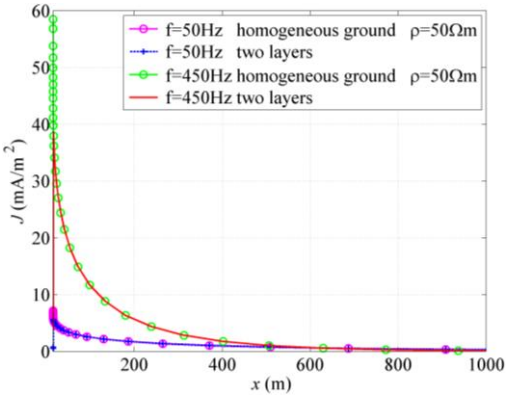

Figure 10

Current distribution inside a two-layer soil, 500 Ωm/50 Ωm, at 50 Hz and at 450 Hz, in a wide range

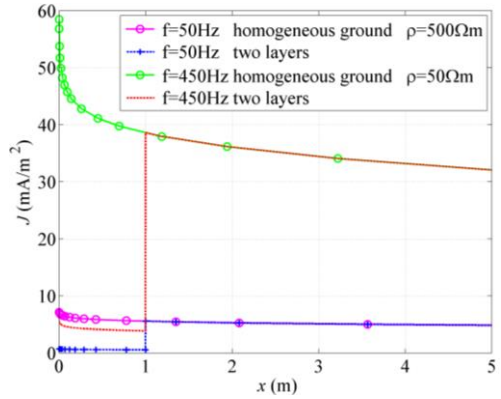

Figure 11

Current distribution inside a two-layer soil, 500 Ωm/50 Ωm, at 50 Hz and at 450 Hz, in a limited range

Distribution of current density vector magnitude, for the same soil resistivity combination, ρ_1/ρ_2 = 500 Ωm/50 Ωm, at 50 Hz, in a limited range, up to the depth of 10 m is presented in Figure 12.

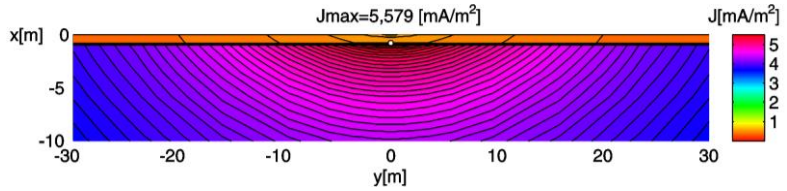

Figure 12

Current distributions inside a two-layer soil, 500 Ωm /50 Ωm, at 50 Hz, up to 10 m inside the ground

Figure 12 demonstrates that the highest value of the current density vector magnitude does not appear at the ground surface, but in the second layer, beyond the separating boundary.

3.3 Penetration Depth

Penetration depth is a measure of how deep any electromagnetic field can penetrate into a material. It is defined as the depth at which the intensity of the field inside the material falls to 1/*e* of its original value at the surface or more properly, just beneath the surface. The penetration depth is a good proxy for the skin effect and is given by the expression [14]:

$$\delta = \sqrt{\frac{2}{\omega\mu\sigma}} = \sqrt{\frac{2\rho}{2\pi f\mu}} = \sqrt{\frac{\rho}{\pi f\mu}}. \tag{20}$$

The penetration depths in meters, for the five most common soil resistivity values in our region and 10 frequencies, are calculated applying (20) and given in Table 2.

Table 2

Penetration Depths in Meters, for Different Soil Resistivity Values and Different Frequencies

f [Hz]	ρ [Ωm]				
	50	250	500	1000	2500
50	503.29	1125.40	1591.55	2250.79	3558.81
100	355.88	795.77	1125.39	1591.55	2516.46
150	290.57	649.75	918.88	1299.49	2054.68
250	225.08	503.29	711.76	1006.58	1591.55
350	190.23	425.36	601.55	850.72	1345.11
500	159.16	355.88	503.29	711.76	1125.40
750	129.95	290.58	410.94	581.15	918.88
1000	112.54	251.65	355.88	503.29	795.77
1500	91.89	205.47	290.58	410.94	649.75
2500	71.18	159.16	225.08	318.31	503.29

Comparing the layer thickness values to the penetration depth values, it can be concluded that the penetration depth is in all cases much higher that the layer thickness.

As also concluded in [15], due to the very small first-layer thickness compared to the penetration depth, the first layer practically has no influence on the current distribution and, consequently, on the ground return impedance. Both cases could be treated as homogeneous cases with the second layer resistivity values. At all observed frequencies, a significant first layer impact can be expected only if the layer thickness varies between 10 m and 50 m [15].

This conclusion is very important, because it enables all following calculations to be performed for the homogeneous soil model, with the resistivity equal to the resistivity of the second layer. It also eliminates the necessity for the complex magnetic field strength vector calculation, applying (18), or numerical integration.

Nevertheless, the calculations of magnetic field strength vector and ground return impedance were performed for both cases; two-layer soil and homogeneous ground by applying numerical integration.

3.4 Ground Return Impedance Calculation

In order to verify the developed method and calculated impedances, the results obtained by this method were also compared to the results obtained by the numerical procedure based on FEM and the results of the simplified Carson's (Carson-Clem) formula for ground return impedance [17].

Numerical procedure based on FEM was performed by applying a computer package COMSOL MULTIPHYSICS', AC/DC Module. For the entire calculation, the mode "2D Quasi-static, Magnetic/Perpendicular Induction Currents, Vector Potential" was chosen, together with the "Time Harmonic" simulation. The calculations were carried out for the two-layer ground.

The simplified Carson's (Carson-Clem) formula for ground current impedance is presented in [17], as:

$$\underline{Z}' = R'_{\mathrm{C}} + 9{,}8696\, f \cdot 10^{-4} + \mathrm{j}\, 2{,}8937\, f \cdot 10^{-3} \log \frac{658{,}86875\sqrt{\frac{\rho}{f}}}{GMR} \ (\Omega / \mathrm{km}) \tag{21}$$

Where:

- R'_{C} is the resistance per unit length of the overhead conductor in Ω/m
- ρ is soil resistivity in Ωm
- f is frequency in Hz
- GMR is effective radius of the overhead conductor in meters

An improved version of (21) is presented in [6].

Expression (21) cannot be applied in the case of a multi-layer or two-layer ground, hence in (21) the single soil resistivity, the resistivity of the lower ground layer, was taken into account.

Ground resistance per unit length, calculated for the soil resistivity combination ρ_1/ρ_2 = 500 Ωm/50 Ωm and d_1 = 1 m is shown in Figure 13. The results of the numerical procedure (FEM) for the same ground parameters are also depicted in Figure 13. The results obtained via (21), denoted as "Carson", are calculated for the homogeneous ground with resistivity value of ρ = 50 Ωm. All three calculations were carried out for the conductor height h = 15 m.

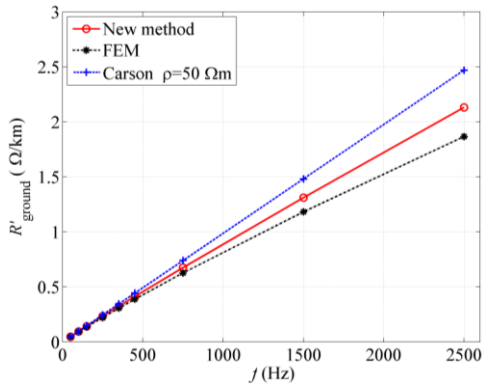

Figure 13
Ground resistance per unit length calculated by applying three different methods

Good agreement of all resistance calculation results is obvious in Figure 13 and this is an excellent verification of the developed method. At the same time, this shows that the simplified formula (21) can be applied for an accurate resistance per unit length determination for two-layer soil as well. This confirms that the simplified expression (21) is still useful, not only for the calculations inside a homogeneous soil, but also for the calculations in any stratified ground with dominant thickness of the lower layer.

Figure 14 displays the relationship between the frequency and the ground reactance per unit length, for a conductor height of h = 15 m, soil resistivity values combination ρ_1/ρ_2 = 500 Ωm/50 Ωm and the results obtained by (21) applied in homogeneous ground, ρ = 50 Ωm. The radius of the overhead conductor is set to be r_c = 0.0144 m.

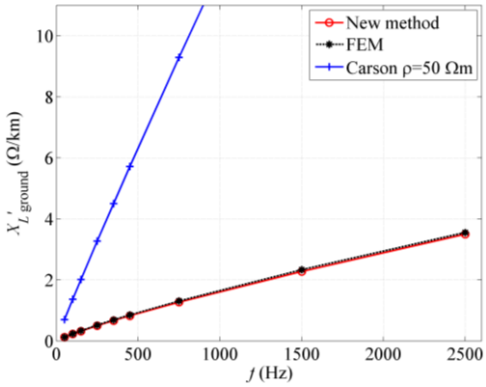

Figure 14
Ground reactance per unit length for h = 15 m and different soil resistivity values, ρ_1/ρ_2 = 500 Ωm/50 Ωm

Comparing the calculated results presented in Figure 14, at the chosen soil resistivity combination $\rho_1/\rho_2 = 500\ \Omega m/50\ \Omega m$, good agreement is seen between the new, analytical, method and the numerical FEM procedure, but not with the simplified "Carson" formula, for the homogeneous ground with resistivity $\rho = 50\ \Omega m$.

Analysis of Figure 14 reveals that the ground reactance per unit length does not increase linearly, but rather slowly with an increasing frequency, predicting that the ground inductance per unit length, will be decreasing with increasing frequency, as expected.

Knowing that the ground return impedance is an inductive load, the ground return inductance can be determined as well. Ground inductance per unit length could be very useful, especially in the case of electromagnetic disturbances on neighboring electronic or telecommunication systems.

Figure 15 depicts ground inductance per unit length as a function of frequency, for a constant conductor height of h = 15 m and soil resistivity values combination $\rho_1/\rho_2 = 500\ \Omega m/50\ \Omega m$ and d_1 = 1 m.

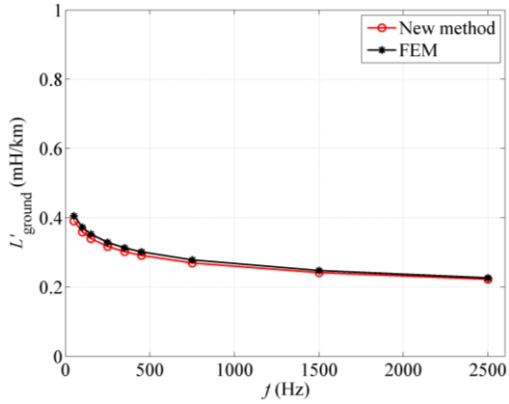

Figure 15

Ground inductance per unit length, for h = 15 m and $\rho_1/\rho_2 = 500\ \Omega m/50\ \Omega m$

The skin effect at lowest frequencies is not significant and ground inductance per unit length has the highest value, decreasing slowly with the increasing frequency. In contrast, at the higher frequencies the skin effect is more pronounced and ground inductance per unit length is at its lowest and decreases even more slowly with the increasing frequency.

In Figure 15, an excellent agreement between the results obtained by the new method and the one obtained by FEM can once again be observed.

The inductances per unit length calculated via the simplified Carson's formula (21) were deemed unreliable and these values are not presented in Figure 15.

Conclusions

In this paper, a novel procedure developed previously for the determination of ground impedance in homogeneous soil, described in detail in [5], was improved, adjusted and applied, for the calculation of the ground return impedance, in a two-layer ground. The inhomogeneous ground was simplified by assuming that ground consists of homogeneous layers, of different thickness, parallel to the surface. The mathematical procedure presented in this paper is also based on a strict electromagnetic approach. The presented method is convenient for an accurate multi-layer ground impedance calculation. The method enables an exact treatment of the skin effect within the multi-layer ground.

The results lead to the most important conclusion: due to the small layer thickness compared to the penetration depth in all investigated cases, all effects are the same as in the case of homogeneous soil, with the resistivity of dipper layers. This conclusion is even more valid in practice, when the thickness of the first layer usually does not exceed a few meters. The distribution of current differs only close to the ground surface, while the differences decrease rapidly in the ground. Hence, the application of the proposed method enables correct calculation of the electric and magnetic fields both in the multi-layer ground and in the space between the conductor and the ground surface.

When the layer thickness is close to the penetration depth (between 10 and 50 m, for low soil resistivity values, at industrial frequency), the suggested magnetic field calculation could be applied, providing an accurate calculation of the ground return impedance. The developed method thus, represents an efficient tool for the multi-layer ground impedance calculations, in electrical power transmission and distribution systems, that include ground return, in which, ground currents have a particular significance. The most common, single line-to-ground fault case can also be successfully treated inside the multi-layer ground.

An excellent agreement between the results of analytical process presented in this paper and the numerical procedure (FEM) was achieved and discussed in this work.

References

[1] Abramowitz M. and Stegun I. A., Eds., "Bessel Functions of Integer Order" in *Handbook of Mathematical Functions*, 9th Ed. New York, NY: Dover Publications, 1970, pp. 355-433

[2] Arnautovski-Toševa V. and Grcev L., "High frequency current distribution in horizontal grounding systems in two-layer soil" in *Proc. 2003 International Symposium on Electromagnetic Compatibility*, pp. 205-208

[3] Kasas-Lazetic K., Prsa M. and Mucalica N., "Current Distribution and Resistance per Unit Length of a Two-Layer Ground" (in Serbian) in *Proc. 2010 International Conf. INFOTEH*, pp. 390-394

[4] Kasas-Lazetic K., Prsa M. and Mucalica N., "Resistance per Unit Length of Homogenous and Two-Layer Ground" (in Serbian) in *Proc. 2010 Conf. on Electrical Distribution Systems of Serbia, CIRED*, pp. 71-75

[5] Kaszás-Lažetić K., Herceg D., Djurić N. and Prša M., "Determining Low-Frequency Earth Return Impedance: A Consistent Electromagnetic Approach" *Acta Polytechnica Hungarica*, 2015, Vol. 12, No. 5, pp. 225-244

[6] Krolo I., Vujević S. and Modrić T., "Highly accurate computation of Carson formulas based on exponential approxiamtion" *Electric Power System Research*, 2018, Vol. 162, pp. 134-141

[7] Ma J., "Fast and high precision calculation of earth return mutual impedance between conductors with a multylayered soil" *COMPEL*, 2018, Vol. 37, No. 3, pp. 1214-1227

[8] Micu D. D., Czumbil L., Prsa M. and Kasas-Lazetic K., "Interfstud electromagnetic interference software - An accurate evaluation of current distribution in soil and in underground pipelines" in *Proc. 2012 International Symposium on Electromagnetic Compatibility*, pp. 1-5

[9] Mucalica D., "Calculation and measurement of characteristic parameters of MV overhead and polyethylene cable systems" M. Sc. thesis, Dept. Elect. Eng., Belgrade Univ., Belgrade, Serbia, 2000 (in Serbian)

[10] Nakagawa M. and Iwamoto K., "Earth-Return Impedance for the Multi-Layer Case" *IEEE Trans. on Power App. Syst*., 1976, Vol. PAS 95, No. 2, pp. 671-676

[11] Olsen R. G. and Willis M. C., "A comparison of exact and quasi-static methods for evaluating grounding systems at high frequencies" *IEEE Trans. Power Del.*, 1996, Vol. 11, No. 2, pp. 1071-1080

[12] Papadopoulos T. A., Papagiannis G. K. and Labridis D. A., "Wave propagation characteristics of overhead conductors above imperfect stratified earth for a wide frequency range" *IEEE Trans. Power Del*., 2009, Vol. 45, No. 3, pp. 1064-1067

[13] Papagiannis G. K., Tsiamitros A., Labridis D. P. and Dokopoulos P. S., "A Systematic approach to the evaluation of the influence of multilayered earth on overhead power transmission lines" *IEEE Trans. Power Del.*, 2005, Vol. 20, No. 4, pp. 2594-2601

[14] Popovic B. D., "Some basic theorems of electromagnetic field" in *Electromagnetics*, 2nd Ed. Belgrade: Gradjevinska knjiga, 1986, p. 52 (in Serbian)

[15] Satsios K. J., Labridis D. P. and Dokopoulos P. S., "The Influence of nonhomogeneous earth on the inductive interference caused to

telecommunication cables by nearby AC electric traction lines", *IEEE Trans. Power Del.*, 2000, Vol. 15, No. 3, pp. 1016-1021

[16] Tsiamitros D. A., Papagiannis G. K. and Dokopoulos P. S., "Equivalent Resistivity Approximation of Two-Layer Earth Structures for Earth return impedances Calculations" in *Proc 2005 Power Tech. IEEE Russia*, pp. 1-7

[17] Write Sh. H. and Hall C. F. (Central Station Engineers of the Westinghouse Electric Corporation), "Characteristics of overhead conductors" in *Electrical Transmission and Distribution - Reference Book*. Pennsylvania East Pittsburgh, 1950, pp. 33-64